Electronic Supplementary Information – Revealing catalytic oxidation mechanism of CO on α-Fe_2O_3 surface: An *ab initio* thermodynamic study

Yun-Hyok Song[a], Yun-Hyok Kye[a,b*], Myong-Il Pang[b], Yong-Min Ho[b], Hyon-Chol Choe[a], Chol-Jun Yu[a*], Chol-Yong Ri[b]

[a]*Computational Materials Design (CMD), Faculty of Materials Science, Kim Il Sung University, Pyongyang, PO Box 76, Democratic People's Republic of Korea*

[b]*Institute of Nanomaterials, Faculty of Materials Science, Kim Il Sung University, Pyongyang, PO Box 76, Democratic People's Republic of Korea*

Correction method for charged defect

Correction energy E_{corr} mainly accounts for the electrostatic interactions between periodically charged supercells with neutralizing background for a computational convergence. As implemented in the Quantum ESPRESSO code [2], the Makov-Payne correction method was used without considering quadrupole moment [3] as follows,

$$E_{\mathrm{corr}}^{\mathrm{MP}} = \alpha q^2/\varepsilon L, \tag{1}$$

where α, ε and L are the Madelung constant, static dielectric constant and supercell lattice constant respectively. The correction energy E_{corr} also should include the band-dispersion correction for shallow defects according to the following equation [1].

$$E_{\mathrm{corr}}^{\mathrm{band}} = \begin{cases} -\sum_k w_k f_k[\epsilon_{\mathrm{CB}}(k) - \epsilon_{\mathrm{CBM}}] & ;\text{shallow donor} \\ \sum_k w_k(1-f_k)[\epsilon_{\mathrm{VB}}(k) - \epsilon_{\mathrm{VBM}}] & ;\text{shallow acceptor} \end{cases} \tag{2}$$

Defect band occupations f_k were taken from the output file of projected density of states (PDOS) calculation and multiplied by their weights w_k. $\epsilon_{\mathrm{VB}}(k)$ ($\epsilon_{\mathrm{CB}}(k)$) is the eigen energy of each k state on fully occupied upper valence band (unoccupied lower conduction band). E_{F} is the Fermi energy, meaning the chemical potential of electron-reservoir with which the defects exchange electrons to be charged differently. The value of E_{F} varies between the valence band maximum (VBM) and the conduction band minimum (CBM) of the perfect bulk material. When a defect is created, E_{F} should represent the potential shift of the reservoir. The potential alignment term ΔV was estimated by comparing deep-lying $3d$ state of Fe atom in the middle fixed layer of the surface slab with the one in bulk material.

*Corresponding author: Yun-Hyok Kye, yh.kye0117@ryongnamsan.edu.kp; Chol-Jun Yu, cj.yu@ryongnamsan.edu.kp

Table S1. Löwdin charge of surface atoms relevant to CO adsorption.

	$Fe\text{-}O_3\text{-}Fe$-			$O_d\text{-}Fe\text{-}O_3$			$O_{2m}\text{-}Fe\text{-}O_3$-			$O_t\text{-}Fe\text{-}O_3$-		
	before	after	Δe	before	after	Δe	before	after	Δe	before	after	Δe
Fe	0.7961	0.5831	-0.2130	0.8118	0.6428	-0.1690	0.7332	0.7354	0.0022	0.6175	0.6470	0.0295
O_3	-0.4598	-0.4558	0.0040	-0.1824	-0.1898	-0.0074	-0.4768	-0.4724	0.0044	-0.3933	-0.3731	0.0202
$O_{d,t,2m}$	-	-	-	-0.2808	-0.3090	-0.0282	0.1671	0.1684	0.0013	-0.1191	-0.1052	0.0139
C(CO)	0.2547	0.4020	0.1473	0.2547	0.4028	0.1481	0.2547	0.2501	-0.0046	0.2547	0.2690	0.0143
O(CO)	-0.0903	-0.0609	0.0297	-0.0903	-0.0545	0.0358	-0.0903	-0.0908	-0.0005	-0.0903	-0.0882	-0.0021

Table S2. Löwdin charge of surface atoms relevant to CO oxidation.

	$Fe\text{-}O_3\text{-}Fe$-			$O_d\text{-}Fe\text{-}O_3$			$O_{2m}\text{-}Fe\text{-}O_3$-			$O_t\text{-}Fe\text{-}O_3$-		
	IS	TS	FS	IS	TS	FS	IS	TS	FS	IS	TS	FS
Fe	0.5831	0.6226	0.5879	0.6428	0.6543	0.7806	0.7354	0.7704	0.6530	0.6470	0.7484	0.7397
$O_{3,d,t,2m}$	-0.4558	-0.4491	-0.1996	-0.3090	-0.2634	-0.2297	0.1684	0.0650	-0.2527	-0.1052	-0.3260	-0.2369
C(CO)	0.4020	0.3865	0.7808	0.4028	0.4426	0.7425	0.2501	0.4018	0.7723	0.2690	0.4073	0.7952
O(CO)	-0.0609	-0.0814	-0.2388	-0.0545	-0.0329	-0.2596	-0.0908	-0.1387	-0.2712	-0.0882	-0.1044	-0.2163

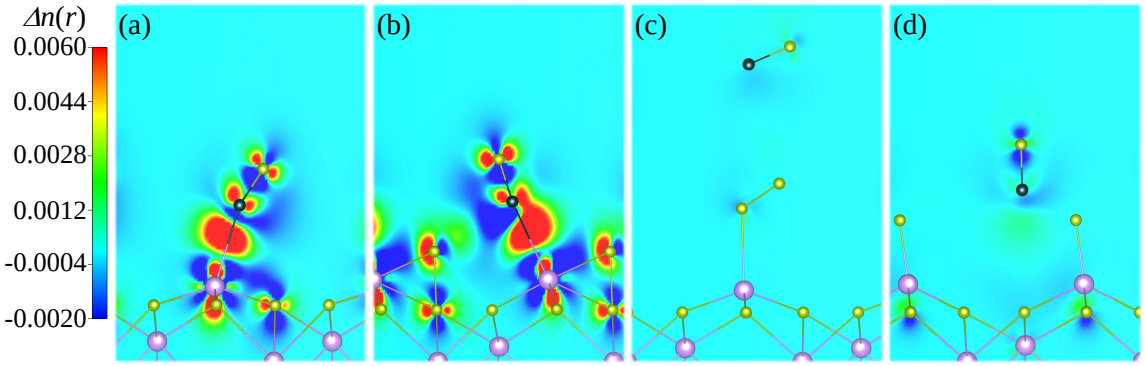

Figure S1. CO adsorption-induced electron charge density variation in Fe_2O_3 (0001) surface with (a) Fe-O_3-Fe-, (b) O_d-Fe-O_3-, (c) O_{2m}-Fe-O_3- and (d) O_t-Fe-O_3- terminations. Positive (negative) value indicates electronic charge accumulation (depletion).

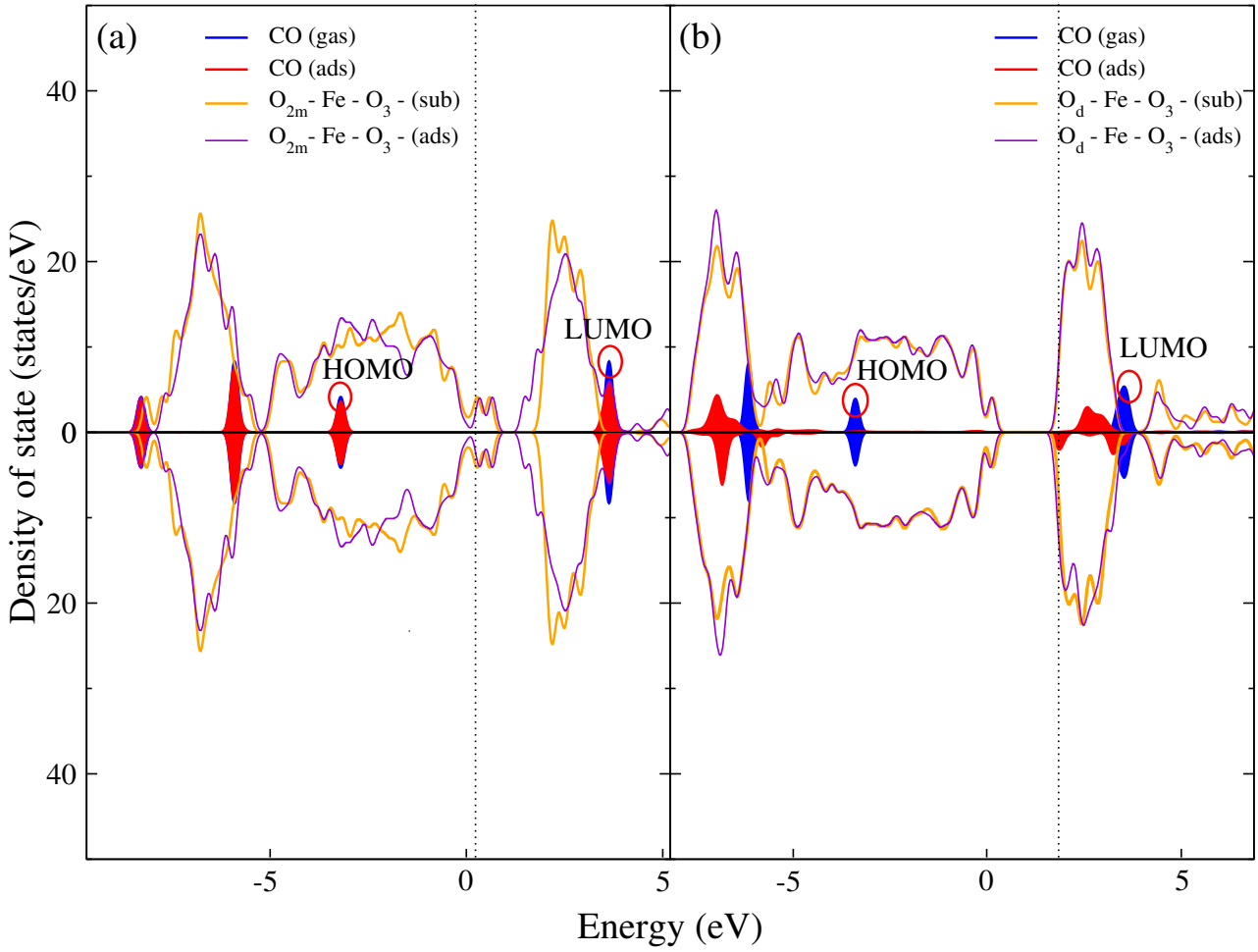

Figure S2. TDOS for spin-up (top panel) and spin-down (bottom panel) states of isolated CO molecule, adsorbed CO molecule, pristine subsrates and CO-adsorbed surfaces with (a) O_{2m}-Fe-O_3- and (b) O_d-Fe-O_3- terminations. The VBM of the bulk phase of α-Fe_2O_3 is set to be zero and the Fermi levels (E_F) of pristine substrates are indicated by vertical dotted lines.

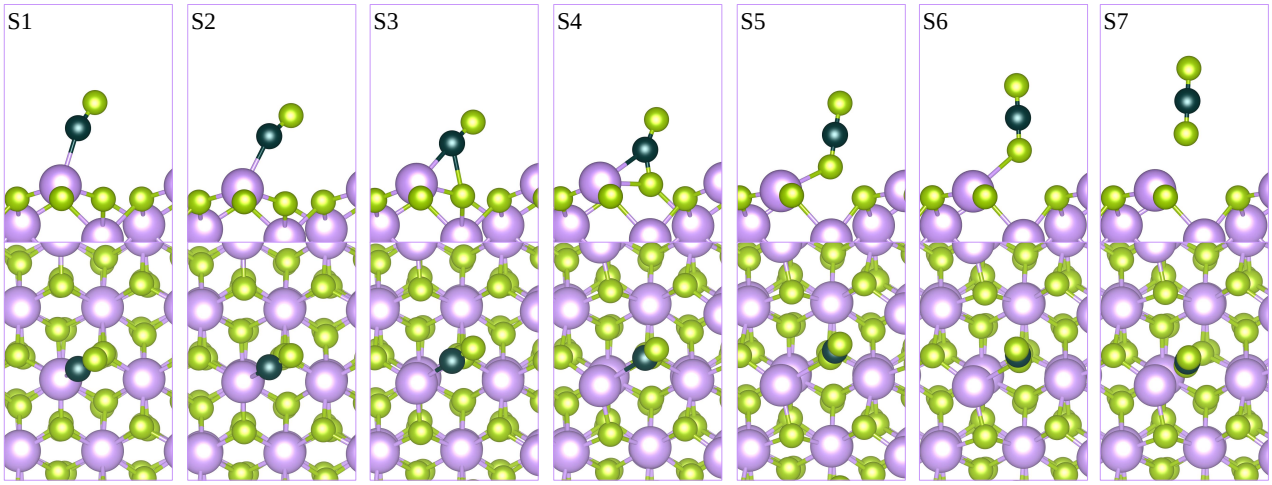

Figure S3. Ball-and-stick view of initial (S1), intermediate (S2-S6) and final (S7) state during CO oxidation to CO_2 on Fe_2O_3 (0001) surface with stoichiometric Fe-O_3-Fe- termination, identified by NEB simulation.

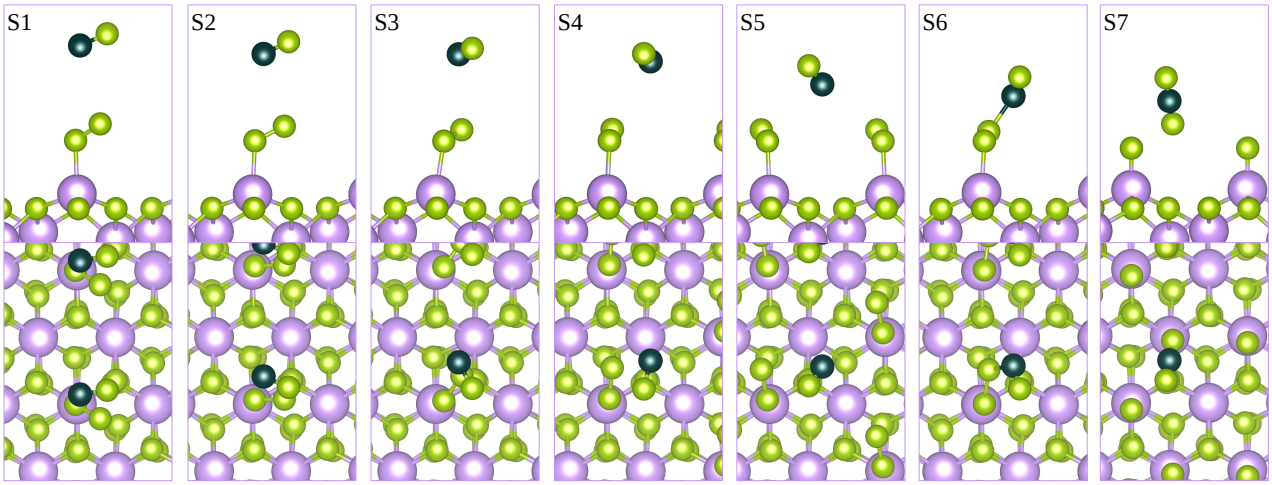

Figure S4. Ball-and-stick view of initial (S1), intermediate (S2-S6) and final (S7) state during CO oxidation to CO_2 on Fe_2O_3 (0001) surface with O_{2m}-Fe-O_3 termination, identified by NEB simulation.

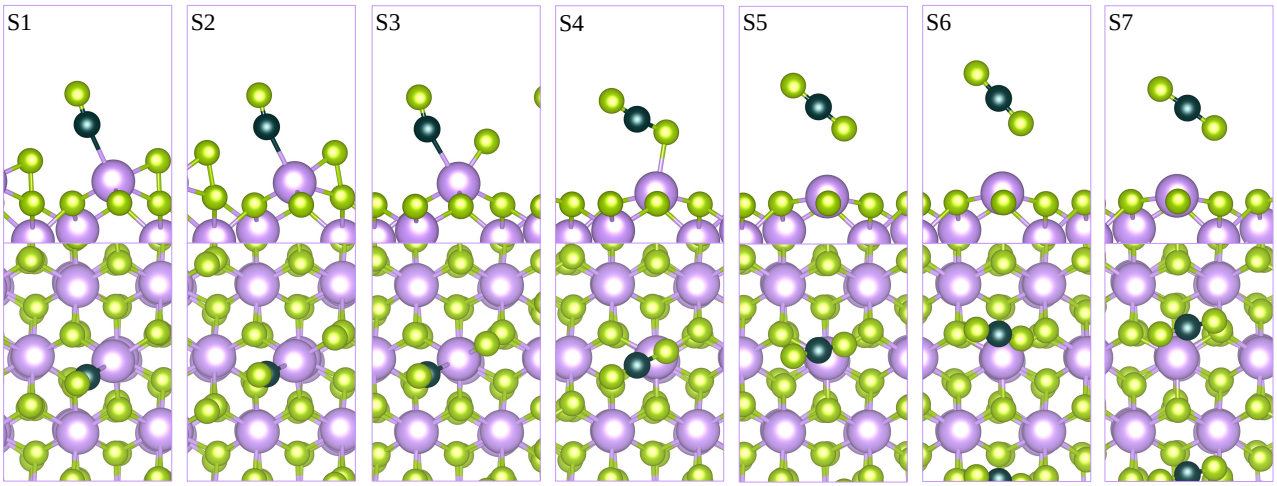

Figure S5. Ball-and-stick view of initial (S1), intermediate (S2-S6) and final (S7) state during CO oxidation to CO_2 on Fe_2O_3 (0001) surface with O_d-Fe-O_3 termination, identified by NEB simulation.

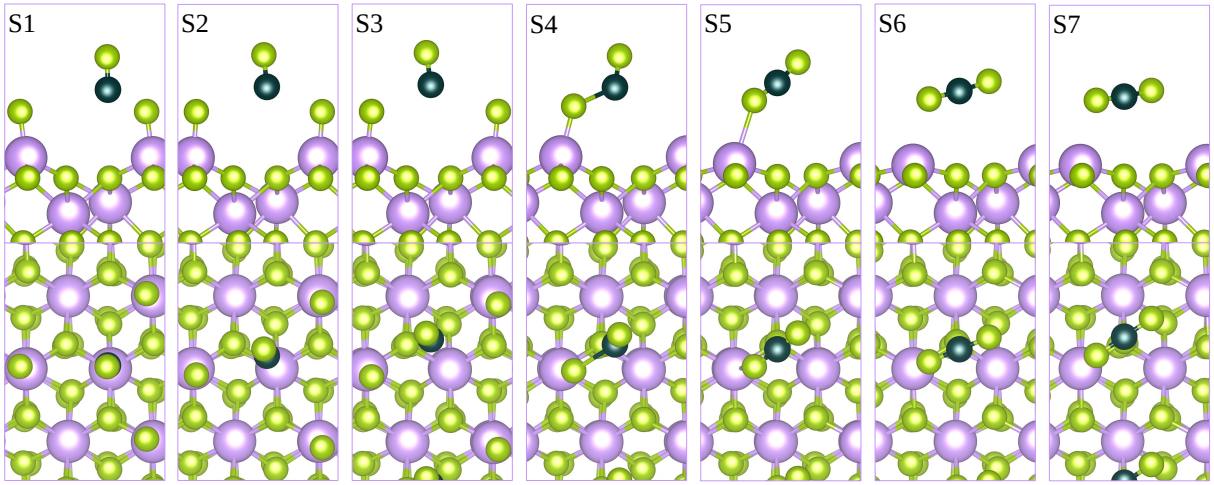

Figure S6. Ball-and-stick view of initial (S1), intermediate (S2-S6) and final (S7) state during CO oxidation to CO_2 on Fe_2O_3 (0001) surface with O_t-Fe-O_3 termination, identified by NEB simulation.

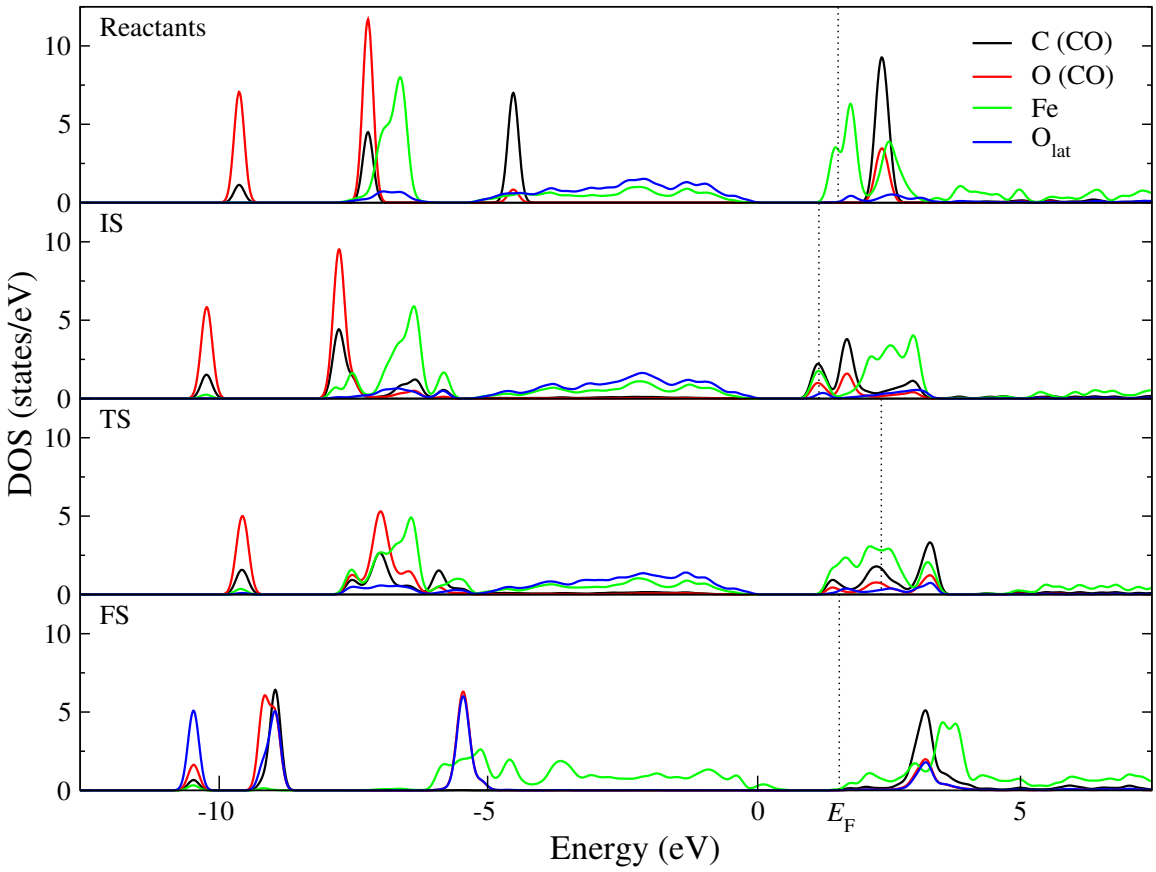

Figure S7. Atom-projected PDOS of stoichiometric Fe-O_3-Fe- terminated surface before CO oxidation and in IS, TS and FS during CO oxidation.

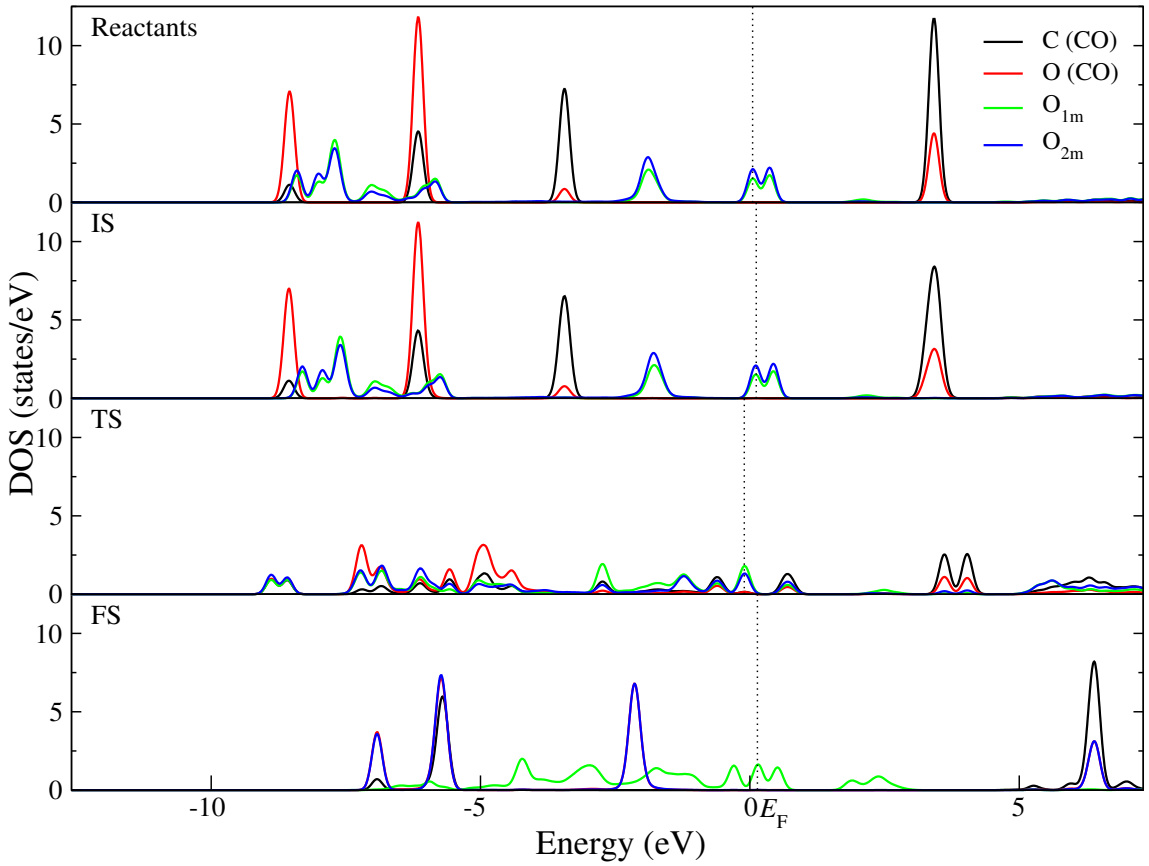

Figure S8. Atom-projected PDOS of O_{2m}-Fe-O_3- terminated surface before CO oxidation and in IS, TS and FS during CO oxidation.

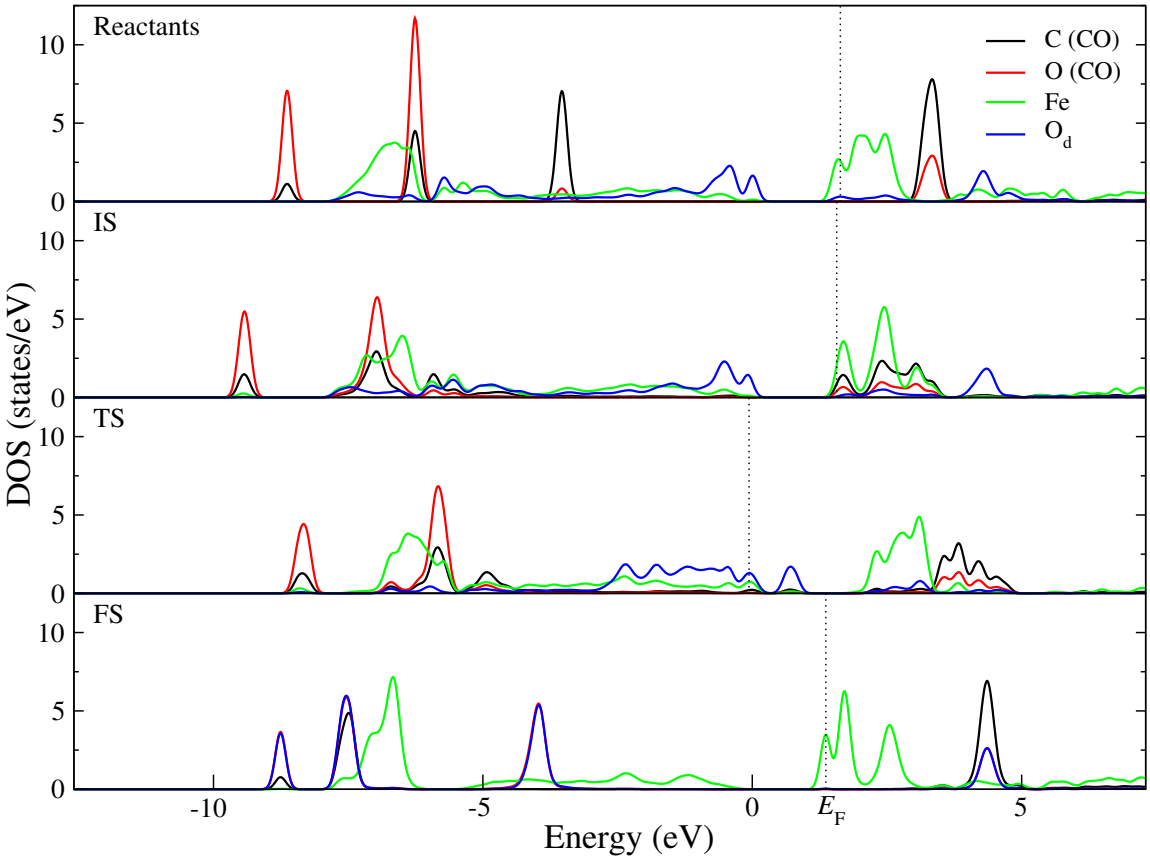

Figure S9. Atom-projected PDOS of O_d-Fe-O_3- terminated surface before CO oxidation and in IS, TS and FS during CO oxidation.

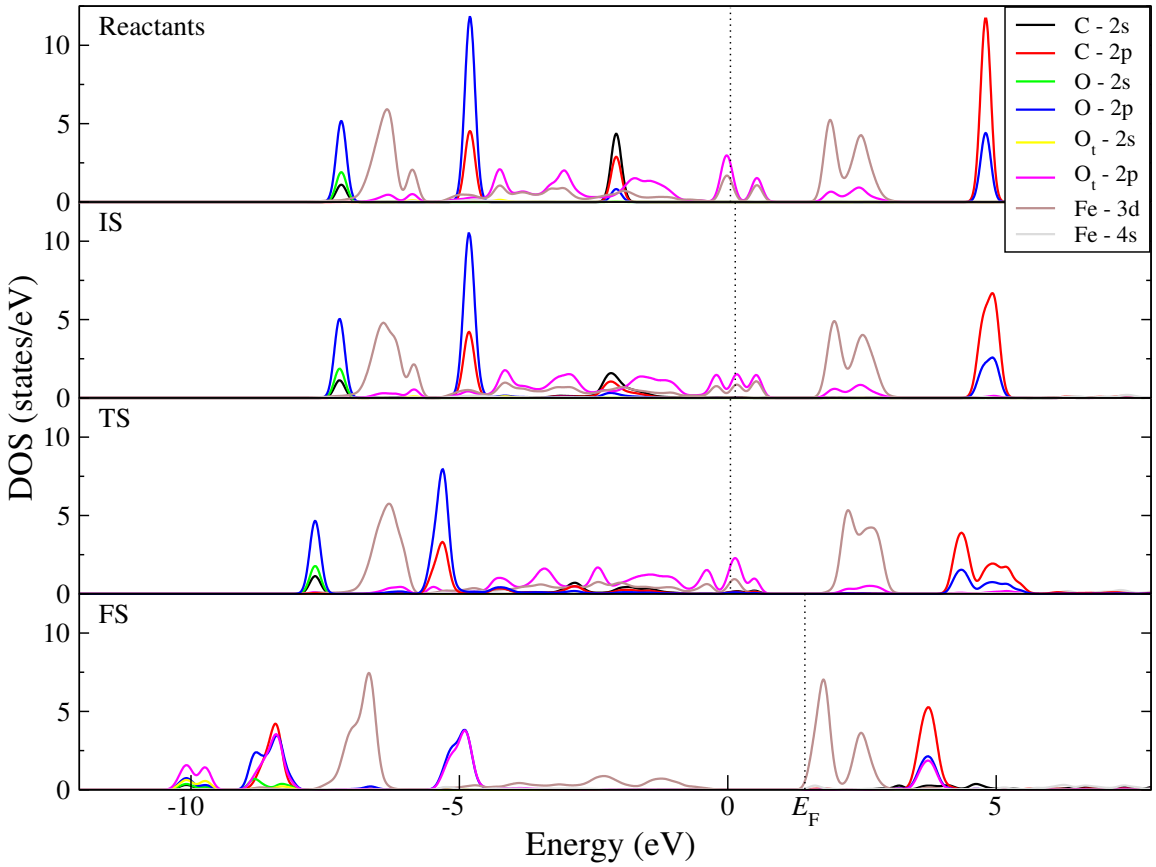

Figure S10. Atomic orbital-projected PDOS of O_t-Fe-O_3- terminated surface before CO oxidation and in IS, TS and FS during CO oxidation.

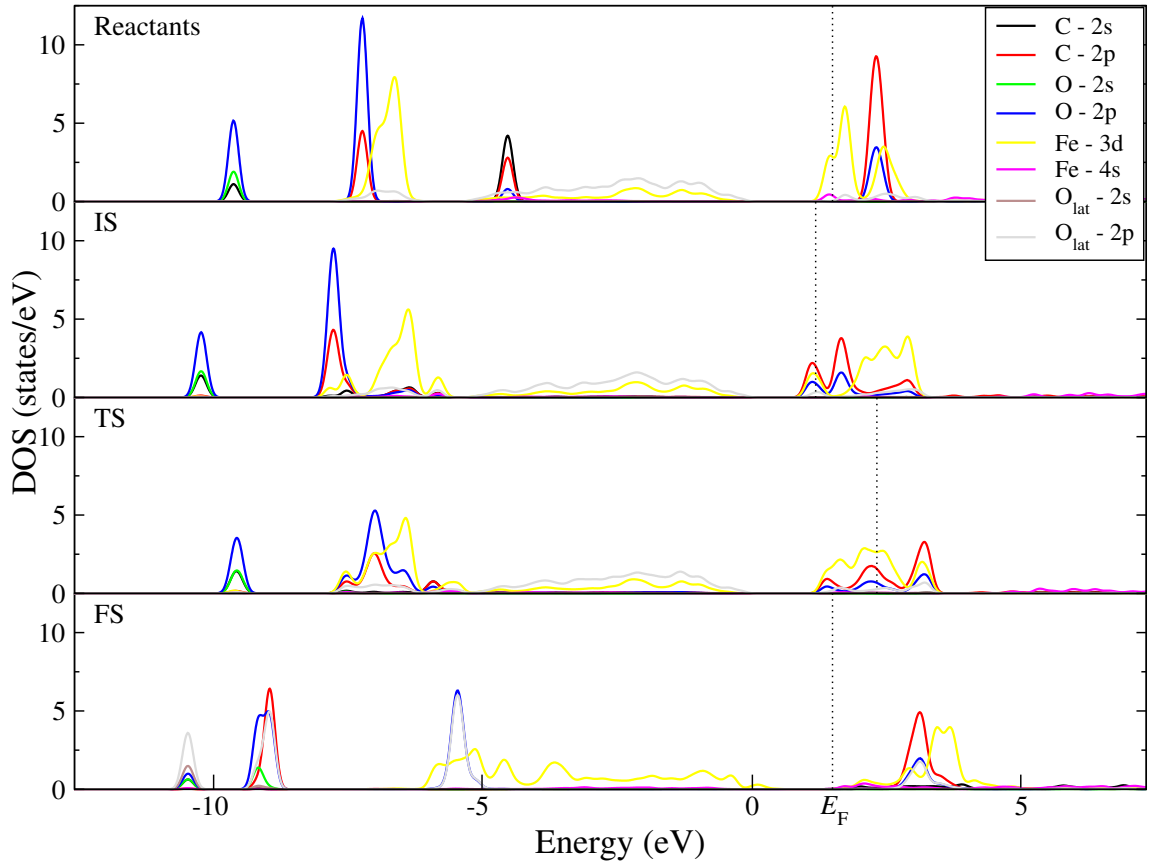

Figure S11. Atomic orbital-projected PDOS of Fe-O_3-Fe- terminated surface before CO oxidation and in IS, TS and FS during CO oxidation.

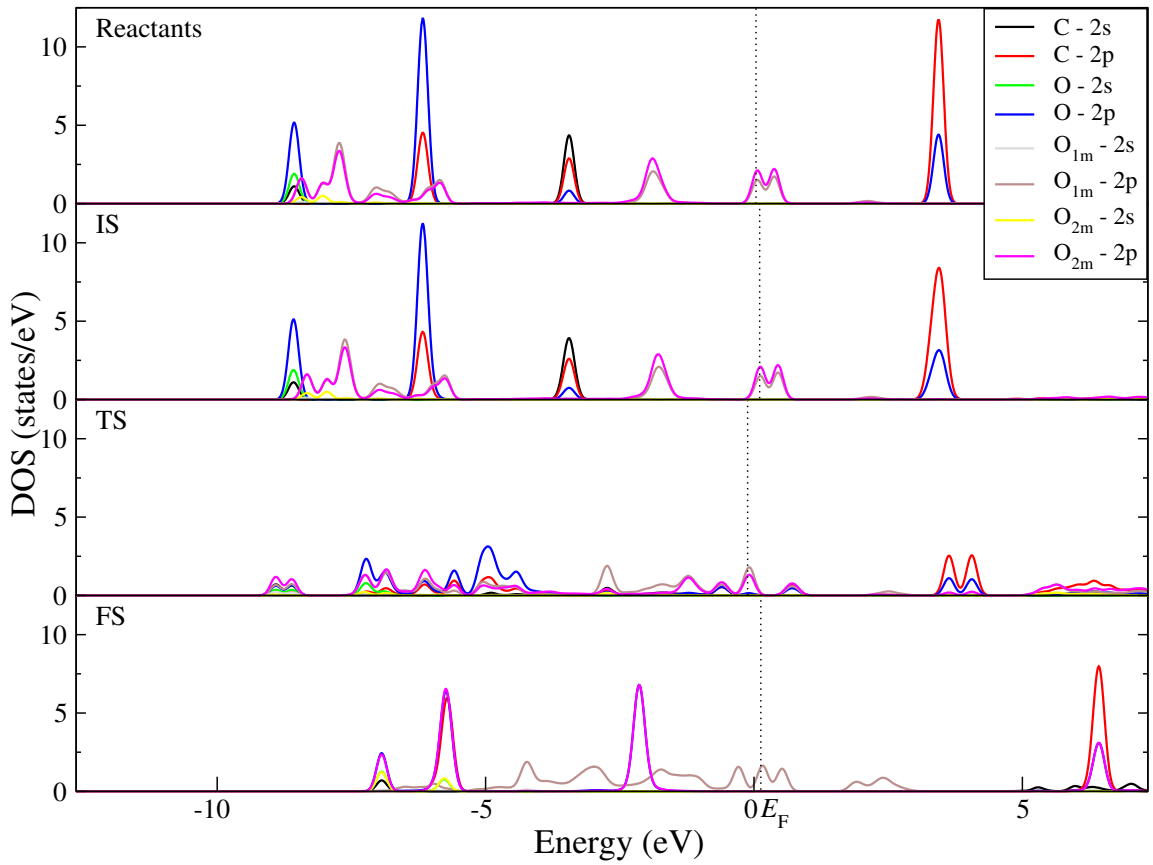

Figure S12. Atomic orbital-projected PDOS of O_{2m}-O_3-Fe- terminated surface before CO oxidation and in IS, TS and FS during CO oxidation.

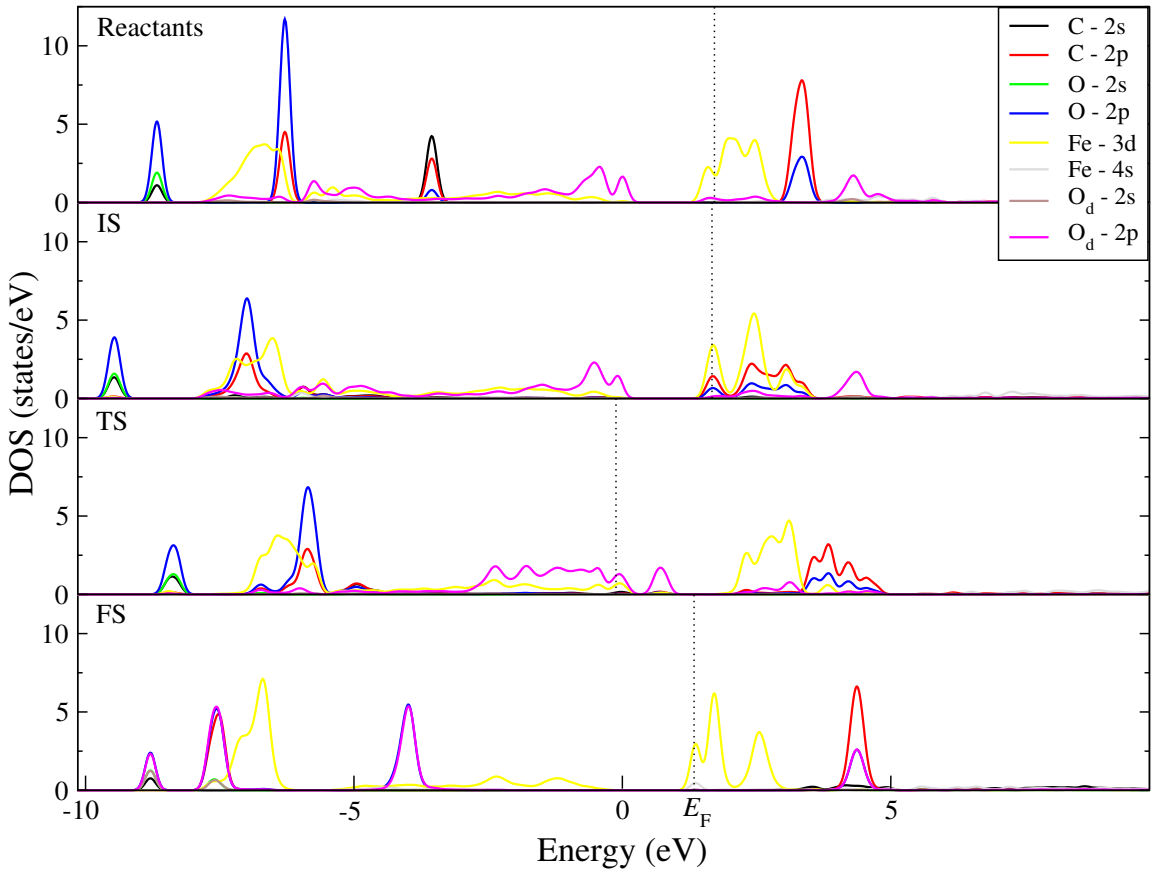

Figure S13. Atomic orbital-projected PDOS of O_d-O_3-Fe- terminated surface before CO oxidation and in IS, TS and FS during CO oxidation.

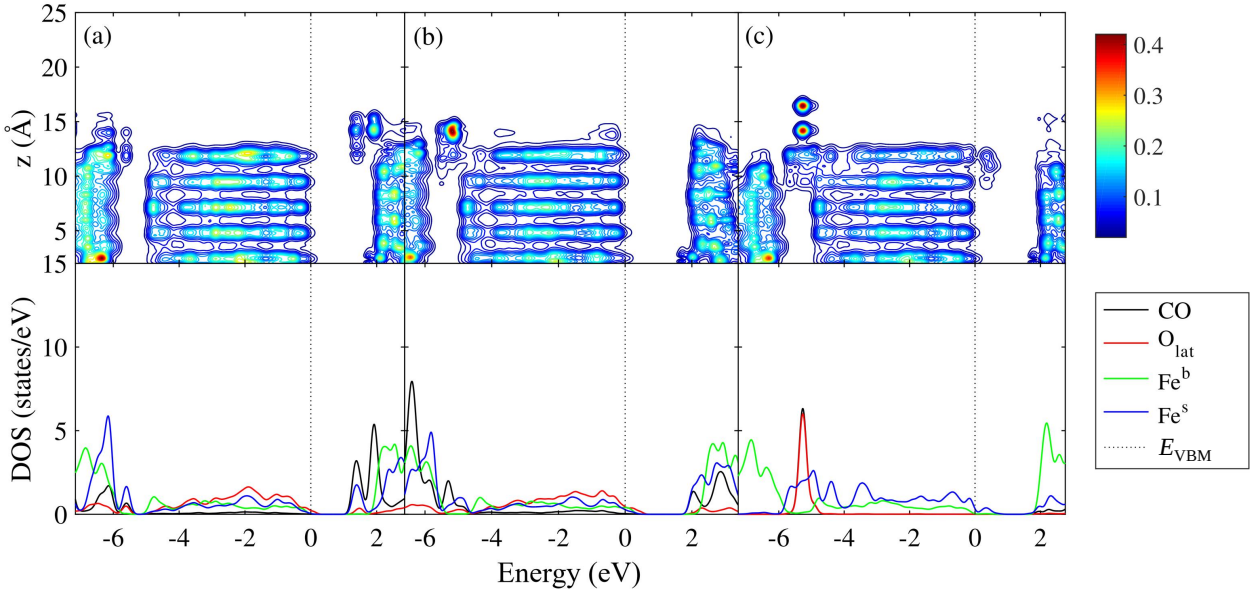

Figure S14. z axis-resolved LDOS (top panel) and atom-projected PDOS of α-Fe_2O_3 (0001) surface with stoichiometric Fe-O_3-Fe- termination in CO oxidation. The VBM of the bulk phase is set to be zero as indicated by vertical dotted lines.

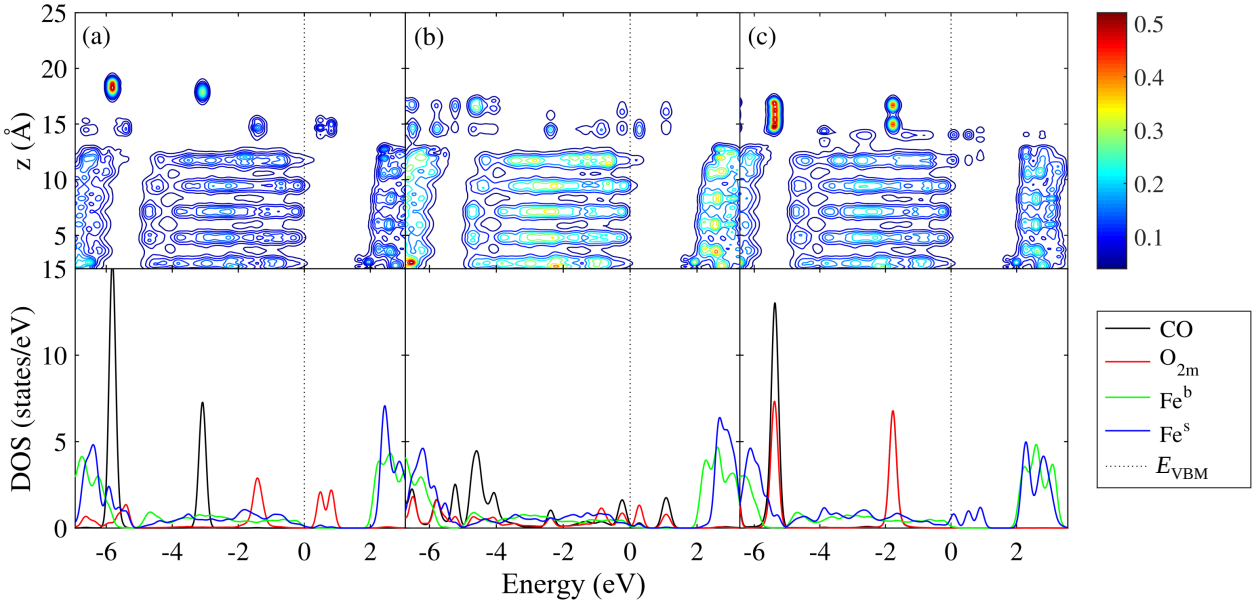

Figure S15. z axis-resolved LDOS (top panel) and atom-projected PDOS of α-Fe_2O_3 (0001) surface with O_{2m}-Fe-O_3- termination in CO oxidation. The VBM of the bulk phase is set to be zero as indicated by vertical dotted lines.

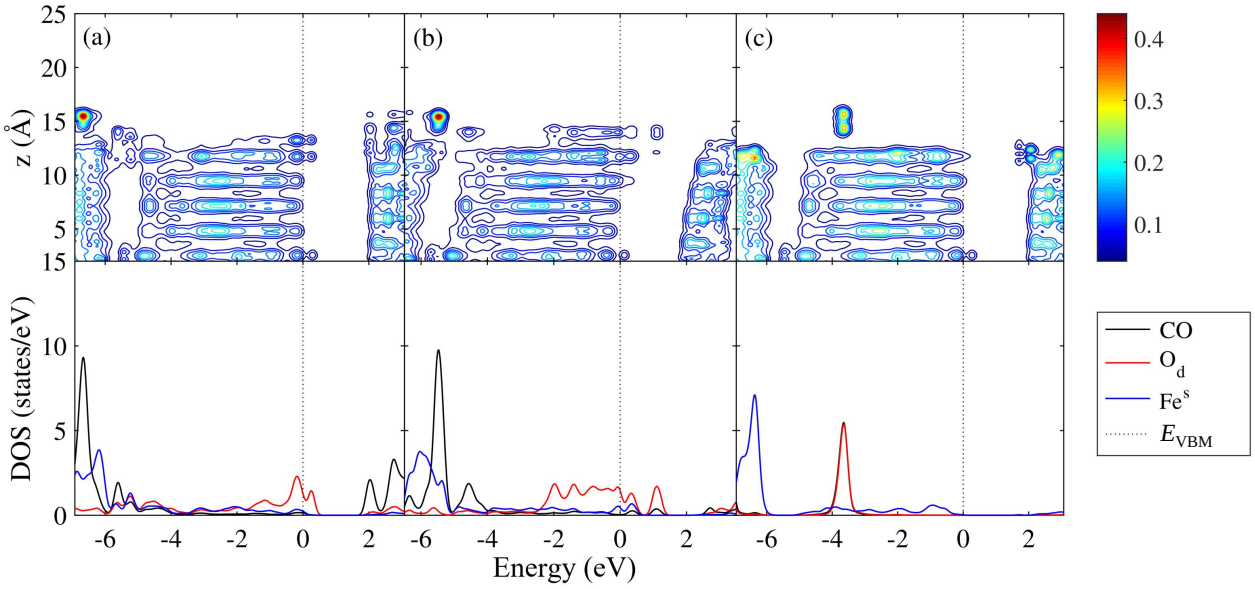

Figure S16. z axis-resolved LDOS (top panel) and atom-projected PDOS of α-Fe_2O_3 (0001) surface with O_d-Fe-O_3- termination in CO oxidation. The VBM of the bulk phase is set to be zero as indicated by vertical dotted lines.

References

[1] C. Freysoldt, B. Grabowski, T. Hickel, J. Neugebauer, G. Kresse, A. Janotti, and C. G. van de Walle. First-principles calculations for point defects in solids. *Rev. Mod. Phys.*, 86:253–305, 2014.

[2] P. Giannozzi, S. Baroni, N. Bonini, M. Calandra, R. Car, C.Cavazzoni, D. Ceresoli, G. L. Chiarotti, M. Cococcioni, I. Dabo, and *et al.* Quantum espresso: A modular and open-source software project for quantum simulations of materials. *J. Phys.: Condens. Matter*, 21:395502, 2009.

[3] G. Makov and M. C. Payne. Periodic boundary conditions in ab initio calculations. *Phys. Rev. B*, 51:4014, 1995.